UCRL- 100879
PREPRINT

A Second-Order Projection Method for the Incompressible Navier Stokes Equations on Quadrilateral Grids

John B. Bell
Lawrence Livermore National Laboratory
Livermore, CA 94550

Jay. M. Solomon
William G. Szymczak
Naval Surface Warfare Center
Silver Spring, MD 20903

This paper was prepared for presentation at the AIAA 9th Computational Fluid Dynamics Conference, Buffalo, New York, June 14-16, 1989.

April 1989

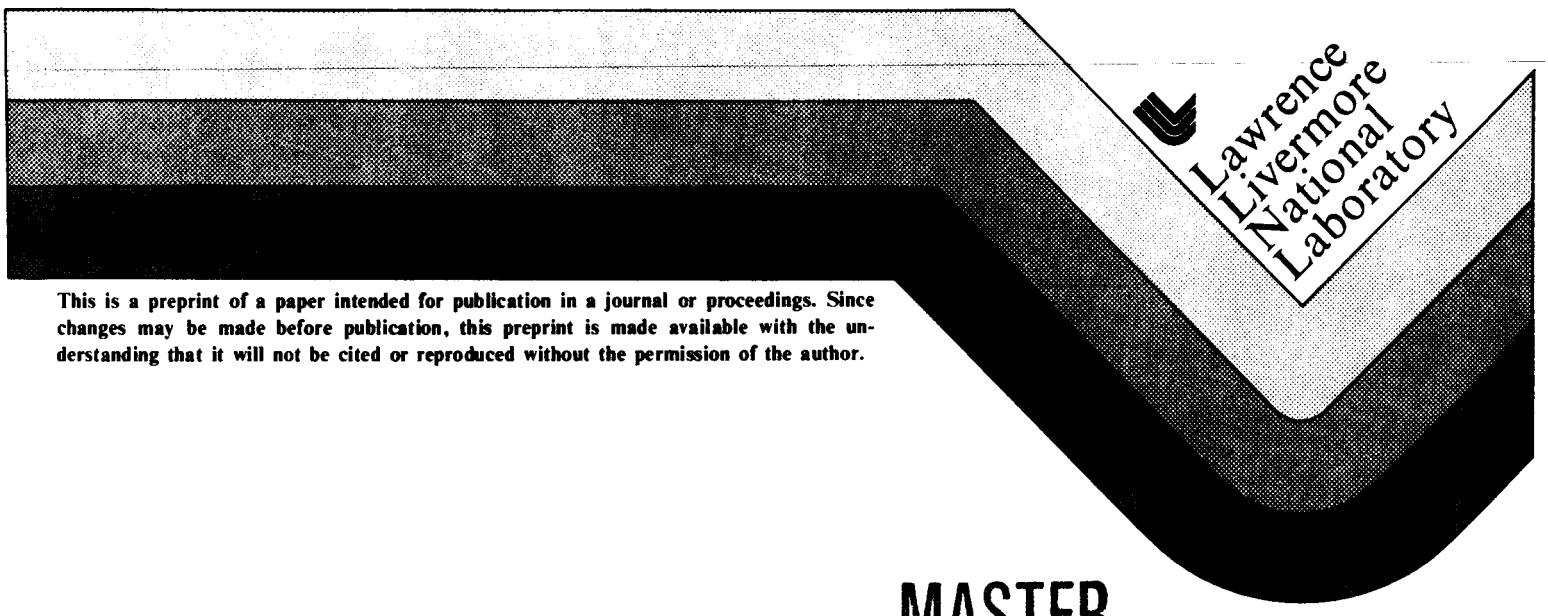

A Second-Order Projection Method for the Incompressible Navier Stokes Equations on Quadrilateral Grids

UCRL--100879

DE89 010242

John B. Bell†
Lawrence Livermore National Laboratory
Livermore, CA 94550

Jay M. Solomon‡§
Naval Surface Warfare Center
Silver Spring, MD 20903

William G. Szymczak‡
Naval Surface Warfare Center
Silver Spring, MD 20903

Abstract

This paper describes a second-order projection method for the incompressible Navier-Stokes equations on a logically-rectangular quadrilateral grid. The method uses a second-order fractional step scheme in which one first solves diffusion-convection equations to predict intermediate velocities which are then projected onto the space of divergence-free vector fields. The spatial discretization of the diffusion-convection equations is accomplished by formally transforming the equations to a uniform computational space. The diffusion terms are then discretized using standard finite-difference approximations. The convection terms are discretized using a second-order Godunov method that provides a robust discretization of these terms at high Reynolds number. The projection is approximated using a Galerkin procedure that uses a local basis for discretely divergence-free vector fields. Numerical results are presented illustrating the performance of the method.

Introduction

This paper describes a second-order projection method for the time-dependent, incompressible Navier-Stokes equations

$$U_t + (U\cdot\nabla)\, U = \varepsilon\Delta U - \nabla p \qquad (1.1)$$

$$\nabla\cdot U = 0 \qquad (1.2)$$

on a logically-rectangular quadrilateral grid where $R_e = 1/\varepsilon$ is the Reynolds number. The method is a generalization of a second-order projection method first introduced by Bell, Colella and Glaz Bell colella viscous bell glaz equations and subsequently developed by Bell et. al. Bell Shear for the study of shear flows. The basic approach is a second-order fractional step method, similar to a method introduced by van Kan Kan in which (1.1) is solved with the pressure term lagged to determine an intermediate velocity field that does not satisfy (1.2). This intermediate velocity field is then decomposed into solenoidal and gradient components which determine the new velocity and an update for the pressure, respectively. The method also incorporates second-order Godunov-type differencing of the nonlinear terms in (1.1) that provides a robust, high-resolution discretization at high Reynolds number.

In deriving the extension to quadrilateral grids we will formally assume that the grid points are defined by a transformation Φ from a computational space $\Xi = (\xi,\eta)$ to the physical space $X = (x,y)$; i.e.,

$$X = \Phi(\Xi) \quad .$$

When we transform the Navier-Stokes equations to the computational coordinate system we obtain

$$JU_t + [\bar{U}\cdot\nabla_\Xi]\, U = \varepsilon\nabla_\Xi\cdot\left(\frac{1}{J}TT^t\nabla_\Xi U\right) - T^t\nabla_\Xi p \qquad (1.3)$$

$$\nabla_\Xi\cdot\bar{U} = 0 \quad . \qquad (1.4)$$

where $J = \det\nabla_\Xi\Phi$, $\bar{U} = TU$ and

$$T \equiv J\,[\nabla_\Xi\Phi]^{-1} = \begin{bmatrix} y_\eta & -x_\eta \\ -y_\xi & x_\xi \end{bmatrix}$$

Here, ∇_Ξ and $\nabla_\Xi\cdot$ denote the gradient and divergence operators in computational space. The quadrilateral-grid

† This work of this author was performed under the auspices of the U.S. Department of Energy by the Lawrence Livermore National Laboratory under contract No. W-7405-Eng-48. Partial support under contract No. W-7405-Eng-48 was provided by the Applied Mathematical Sciences Program of the Office of Energy Research.

‡ The work of these authors was supported by the NSWC Independent Research Fund.

§ Member, AIAA.

tions (1.3) and (1.4). The metric coefficients introduced in the transformation are evaluated using appropriate differences of grid-point locations. These difference approximations are chosen so that the method satisfies a free-stream preservation property that guarantees exact treatment of a uniform flow independent of the grid variation. The algorithm is designed to be second-order accurate for smooth flow provided the mapping Φ is smooth. The higher-order Godunov treatment of the convective terms and free-stream preservation ensure the robustness of the algorithm for rough data and for nonsmooth grid variation. We emphasize that the algorithm does not explicitly use the mapping Φ; all that is actually required are the locations of the grid points in physical space. Consequently, an elliptic grid generation algorithm can be used to generate the grids.

In the next section we describe the basic fractional-step approach used for the temporal discretization in the algorithm. In section three, we discuss the spatial discretization of the diffusion-convection equation (1.3) and in section four we describe the discrete Galerkin algorithm for approximating the projection. In the last section we present computational results for flow in a channel with a constriction and flow over a cylinder.

Temporal discretization

In this section we describe the second-order fractional step formulation used in the quadrilateral-mesh projection algorithm. This formulation, which provides the basic temporal discretization, is the same as that used by Bell, Colella and Glaz [2]. Projection methods, originally developed by Chorin [5], are fractional step methods based on the decomposition of vector fields into a divergence-free component and the gradient of a scalar field. More precisely, any vector field V can be uniquely written as $V = U_d + \nabla\phi$ where ϕ is a scalar and U_d is divergence free and satisfies specified boundary conditions. Furthermore, one can define an orthogonal projection $\mathbf{P}$ such that $U_d = \mathbf{P}V$ and $\nabla\phi = (\mathbf{I}-\mathbf{P})V$. (See Temam [6] for a more detailed discussion of the projection.) The algorithm will be defined in terms of the computational space where the vector-field decomposition becomes

$$V = U_d + J^{-1}T^t\nabla_\Xi\phi$$

where U_d satisfies (1.4).

Using the projection we can rewrite the Navier-Stokes equations (1.3)-(1.4) in the equivalent form

$$U_t = \mathbf{P}\left[J^{-1}(\varepsilon\nabla_\Xi\cdot(\frac{1}{J}TT^t\nabla_\Xi U) - [\overline{U}\cdot\nabla_\Xi]\,U)\right] \quad (2.1)$$

Equation (2.1) describes the evolution of U in terms of a nonlinear functional of U; the pressure has been eliminated from the system. Thus, the pressure in (1.3)-(1.4) represents the gradient component of the vector field that is projected in (2.1); i.e.,

$$J^{-1}T^t\nabla_\Xi p = (\mathbf{I}-\mathbf{P})\left[\frac{1}{J}\left[\varepsilon\nabla_\Xi\cdot(\frac{1}{J}TT^t\nabla_\Xi U)-[\overline{U}\cdot\nabla_\Xi]\,U\right]\right]$$

For the basic temporal discretization, we assume that we are given an approximation to U^n. Furthermore, we assume that we have already computed a second-order time-centered approximation to the nonlinear terms $[(\overline{U}\cdot\nabla)U]^{n+\frac{1}{2}}$. (A Godunov-type procedure for computing this approximation is described in the next section.) A straightforward second-order discretization (2.1) can be obtained using a Crank-Nicholson approximation

$$\frac{U^{n+1}-U^n}{\Delta t} = \mathbf{P}\left[\frac{1}{J}\left[\frac{\varepsilon}{2}\nabla_\Xi\cdot(J^{-1}TT^t\nabla_\Xi(U^n+U^{n+1}))-[(\overline{U}\cdot\nabla)U]^{n+\frac{1}{2}}\right]\right] \quad (2.2)$$

However, the linear algebra problem associated with solving (2.2) would be extremely costly because of the nonlocal behavior of the projection.

As a less costly alternative, we construct a fractional step method that approximates (2.2) to second-order accuracy. To accomplish this we will assume that we are also given an approximation to $J^{-1}T^t\nabla_\Xi p^{n-\frac{1}{2}}$. We then compute an intermediate velocity field U^* using

$$J\frac{U^*-U^n}{\Delta t}+T^t\nabla p^{n-\frac{1}{2}} = \frac{\varepsilon}{2}\nabla_\Xi\cdot(J^{-1}TT^t\nabla_\Xi(U^n+U^*))-[(\overline{U}\cdot\nabla)U]^{n+\frac{1}{2}} \quad (2.3)$$

where U^* satisfies the same boundary conditions as U. The role the the pressure gradient term in (2.3) is to approximate the effect of the projection in (2.2). We now apply the projection to decompose U^* into divergence-free and gradient components to obtain U^{n+1} and an update for ∇p

$$U^{n+1} = \mathbf{P}U^* \quad (2.4a)$$

$$J^{-1}T^t\nabla_\Xi p^{n+\frac{1}{2}} = J^{-1}T^t\nabla_\Xi p^{n-\frac{1}{2}} + \Delta t^{-1}(\mathbf{I}-\mathbf{P})U^* \quad (2.4b)$$

Equations (2.3)-(2.4) represent the fractional step scheme that we have used. The relationship between (2.3)-(2.4) and the Crank-Nicholson scheme (2.2) can be seen by first observing that (2.4) is equivalent to

$$\frac{U^{n+1}-U^n}{\Delta t} = \mathbf{P}\left[\frac{U^*-U^n}{\Delta t} + J^{-1}T^t\nabla_\Xi p^{n-\frac{1}{2}}\right] \quad (2.5a)$$

$$J^{-1}T^t\nabla p^{n+\frac{1}{2}} = (\mathbf{I}-\mathbf{P})\left[\frac{U^*-U^n}{\Delta t} + J^{-1}T^t\nabla_\Xi p^{n-\frac{1}{2}}\right] \quad (2.5b)$$

If we use equation (2.3) to replace

$$\frac{U^*-U^n}{\Delta t} + J^{-1}T^t\nabla_\Xi p^{n-\frac{1}{2}}$$

in (2.5) we obtain

$$\frac{U^{n+1}-U^n}{\Delta t} =$$

$$\mathbf{P}\left[\frac{1}{J}\left[\frac{\varepsilon}{2}\nabla_\Xi\cdot(J^{-1}TT^t\nabla_\Xi(U^n+U^*))-[(\overline{U}\cdot\nabla)U]^{n+\frac{1}{2}}\right]\right]$$

$$J^{-1}T^t\nabla p^{n+\frac{1}{2}} =$$

$$(\mathbf{I}-\mathbf{P})\left[\frac{1}{J}\left[\frac{\varepsilon}{2}\nabla_\Xi\cdot(J^{-1}TT^t\nabla_\Xi(U^n+U^*))-[(\overline{U}\cdot\nabla)U]^{n+\frac{1}{2}}\right]\right]$$

from which we can see that (2.4a) corresponds to (2.2) with U^{n+1} approximated by U^* on the right hand side and that $J^{-1}T^t\nabla_\Xi p^{n+\frac{1}{2}}$ represents the gradient component of the vector field being projected.

We note that since $\nabla p^{-\frac{1}{2}}$ is not available, some procedure is required to initialize the fractional step algorithm. We have chosen to simply iterate (2.3) and (2.4) (with $\nabla p = 0$ initially) on the first step to compute converged approximations to U^1 and $J^{-1}T^t\nabla_\Xi p^{\frac{1}{2}}$.

The inclusion of the $J^{-1}T^t\nabla_\Xi p^{n-\frac{1}{2}}$ in (2.3) makes the algorithm second-order accurate in time. The reader is referred to Bell, Colella and Glaz [1] for a more detailed discussion of the convergence behavior of the fractional step scheme. There are several alternative formulations that also give second-order temporal accuracy. Van Kan [4] proposes a similar scheme in which the pressures are not staggered in time. Kim and Moin [7] achieve second-order accuracy by modifying the boundary conditions satisfied by U^*.

Before describing the spatial discretizations used in the algorithm we will summarize the basic approach. First we solve the diffusion-convection equations (2.3). This is a two-step process in which we first approximate $[(\overline{U}\cdot\nabla)U]^{n+\frac{1}{2}}$ using a second-order Godunov procedure. Then, we solve the two parabolic equations represented by (2.3) with the nonlinear term treated as a source term. In the second step of the algorithm, we apply the projection to update U and $J^{-1}T^t\nabla_\Xi p$. In the next section we discuss the spatial discretization of the diffusion-convection equations that forms the first step of the algorithm. In the following section we describe the approximation of the projection.

Spatial discretization

The spatial discretization is based on the staggered grid system depicted in Figure 1. On this grid, vector quantities (U and ∇p) are defined at the grid points, denoted by • in the figure, and scalar quantities ($\nabla\cdot U$ and p) are defined at the cell centers, denoted by × in the figure. The transformation Φ is viewed as being defined so that the grid in computational space is composed of unit squares; i.e., $X_{ij} = \Phi(i,j)$. (Thus, the grid in computational space has $\Delta\xi = \Delta\eta = 1$ so that difference approximations are undivided.) The cell centers $X_{i+\frac{1}{2},j+\frac{1}{2}} = \frac{1}{4}(X_{ij} + X_{i+1,j} + X_{i,j+1} + X_{i+1,j+1})$ form a dual grid that associates a cell with each of the original grid-points. Differences of the dual grid point locations are used to define metric coefficients on the primary grid, namely,

$$X_{\xi,ij} = \tfrac{1}{2}(X_{i+\frac{1}{2},j+\frac{1}{2}}+X_{i+\frac{1}{2},j-\frac{1}{2}}-X_{i-\frac{1}{2},j+\frac{1}{2}}-X_{i-\frac{1}{2},j-\frac{1}{2}})$$

with an analogous formula for $X_{\eta,ij}$. We note that this particular choice of difference approximations for the metric coefficients, although not unique, is not arbitrary. For example, using simple centered difference approximations fails to yield an algorithm that is free-stream preserving.

As noted above there are two distinct components of the spatial approximation of (2.3): discretization of the Laplacian used to model the diffusion terms and the second-order Godunov procedure that is used to compute $[(\overline{U}\cdot\nabla)U]^{n+\frac{1}{2}}$. The discretization of the Laplacian is done using standard, finite difference approximations. The Laplacian in computational coordinates, namely $\nabla_\Xi\cdot(J^{-1}TT^T\nabla_\Xi U)$, has the form

$$(\alpha U_\xi)_\xi + (\beta U_\xi)_\eta + (\beta U_\eta)_\xi + (\gamma U_\eta)_\eta \qquad (3.1)$$

where

$$\alpha = J^{-1}(x_\eta^2 + y_\eta^2)\ ,\ \beta = -J^{-1}(x_\eta y_\xi + x_\xi y_\eta)\ ,$$
$$\text{and } \gamma = J^{-1}(x_\xi^2 + y_\xi^2)\ .$$

Each term in (3.1) is discretized using standard second-order differences with coefficients computed by averaging metric coefficients at grid points. The linear system associated with the parabolic equations (2.3) using (3.1) for the diffusion discretization is solved using diagonal scaling as a preconditioner for conjugate gradient iteration.

The algorithm for computing of $[(\overline{U}\cdot\nabla)U]^{n+\frac{1}{2}}$ is based on the unsplit, second-order upwind methods first proposed by Colella [8] and by van Leer [9]. Unlike standard upwind differencing methods, these types of schemes couple the spatial and temporal discretization by propagating information along characteristics. This approach leads to a robust higher-order discretization with excellent phase-error properties. The scheme described here is a cell-centered predictor-corrector scheme. We use the cells defined by the dual grid for the discretization. In the predictor step of the algorithm, we extrapolate U along characteristics to obtain values at the cell edges at $t^{n+\frac{1}{2}}$. In the corrector step we compute upwind fluxes for the velocities which are then differenced to obtain a time-centered approximation to $(\overline{U}\cdot\nabla)U$.

Predictor

In the predictor we extrapolate along characteristics using solution values at t^n to predict values of U on cell edges at time $t^{n+\frac{1}{2}}$. The basis for the extrapolation is Taylor series. To second order accuracy

$$U^{n+\frac{1}{2},L}_{i+\frac{1}{2},j} = U^n_{ij} + \frac{1}{2}U^n_{\xi,ij} + \frac{\Delta t}{2}U^n_{t,ij} \qquad (3.2a)$$

$$U^{n+1/2,R}_{i-1/2,j} = U^n_{ij} - \frac{1}{2}U^n_{\xi,ij} + \frac{\Delta t}{2}U^n_{t,ij} \qquad (3.2b)$$

$$U^{n+1/2,B}_{i,j+1/2} = U^n_{ij} + \frac{1}{2}U^n_{\eta,ij} + \frac{\Delta t}{2}U^n_{t,ij} \qquad (3.2c)$$

$$U^{n+1/2,T}_{i,j-1/2} = U^n_{ij} - \frac{1}{2}U^n_{\eta,ij} + \frac{\Delta t}{2}U^n_{t,ij} \ . \qquad (3.2d)$$

The first two quantities denote the extrapolation of U to the left side of edge-$i+\frac{1}{2},j$ and to the right side of edge-$i-\frac{1}{2},j$, respectively. The last two are the extrapolation of U to the bottom side of edge-$i,j+\frac{1}{2}$ and the top side of edge-$i,j-\frac{1}{2}$. We now use the differential equations (1.3) to express the time derivatives in terms of spatial derivatives with the pressure gradient lagged to time $t^{n-1/2}$. This gives, for (3.2a)

$$U^{n+1/2,L}_{i+1/2,j} = U^n_{ij} + s_L\left(\frac{1}{2} - \frac{\Delta t}{2J}\bar{u}^n_{ij}\right)U^n_{\xi,ij} - \frac{\Delta t}{2J}\bar{v}^n_{ij}U^n_{\eta,ij} + \frac{\Delta t}{2J}\left[\nabla_\Xi\cdot\left(\frac{1}{J}TT^t\nabla_\Xi U\right) - T^t\nabla_\Xi p\right] \qquad (3.3)$$

where s_L is 1 if $\bar{u}^n_{ij} \geq 0$ and 0 otherwise. Analagous formulae are used for (3.2b-d). In (3.3), the derivative normal to the edge, U_ξ, is evaluated using central differences with monotonicity constraints which we denote by $(\Delta_\xi U)_{ij}$. The transverse derivative is evaluated using an upwind difference approximation. More precisely, if $\bar{v}_{ij} \geq 0$

$$U_{\eta,ij} = U_{ij} - U_{ij-1} + \left(\frac{1}{2} - \frac{\Delta t\,\bar{v}_{ij}}{2J}\right)\left[(\Delta_\eta U)_{ij} - (\Delta_\eta U)_{ij-1}\right]$$

or, if $\bar{v}_{ij} < 0$

$$U_{\eta,ij} = U_{ij+1} - U_{ij} - \left(\frac{1}{2} + \frac{\Delta t\,\bar{v}_{ij}}{2J}\right)\left[(\Delta_\eta U)_{ij+1} - (\Delta_\eta U)_{ij}\right]$$

where $\Delta_\eta U$ denotes a monotonized central difference approximation in the η-direction with all quantities evaluated at t^n.

Corrector

In the corrector step we compute $\bar{u}\,U_\xi + \bar{v}\,U_\eta$ from the predicted values defined by (3.3). (For the remainder of this section we suppress $n+\frac{1}{2}$ superscripts.) The form of the corrector is motivated by a physical-space interpretation of the matrix T used to define $\bar{U}$. At edge-$i+\frac{1}{2},j$ $\bar{u} = X_\eta\cdot U$. If we let $X_{\eta,i+1/2,j} = X_{i+1/2,j+1/2} - X_{i+1/2,j-1/2}$ we see that $X_{\eta,i+1/2,j}$ is the normal to the edge, scaled to the length of the edge. Consequently, $\bar{u}_{i+1/2,j}U_{i+1/2,j}$ represents the flux of U through edge-$i+\frac{1}{2},j$. This suggests the following finite volume type differencing for the corrector:

$$\bar{u}\,U_\xi + \bar{v}\,U_\eta \approx \tfrac{1}{2}(\bar{u}_{i+1/2,j} + \bar{u}_{i-1/2,j})(U_{i+1/2,j} - U_{i-1/2,j}) + \tfrac{1}{2}(\bar{v}_{i,j+1/2} + \bar{v}_{i,j-1/2})(U_{i,j+1/2} - U_{i,j-1/2}) \qquad (3.4)$$

where $\bar{u}$ and $\bar{v}$ are the appropriately scaled normal velocities at ξ=constant and η= constant edges, respectively.

Before evaluating the flux we must first resolve the ambiguities in edge values introduced by (3.2). In particular, the characteristic extrapolation has defined double values of U for each edge corresponding to expansions from either side of the interface. We will restrict the discussion to the computation of $\bar{u}_{i+1/2,j}$ and $U_{i+1/2,j}$ for edge-$i+\frac{1}{2},j$ from the left and right states $U^L_{i+1/2,j}$ and $U^R_{i+1/2,j}$. If we transform the Navier-Stokes equations to a local Cartesian coordinate system defined by the edge and its normal we see that $\bar{u}$ satisfies

$$\bar{u}_t + \bar{u}\,\bar{u}_\chi = R \qquad (3.5)$$

where χ is the direction normal to the edge. Here R represents the diffusion term, the pressure gradient and the transverse flux. Thus, $\bar{u}$ satisfies the quasilinear form of Burgers' equation with forcing terms in the direction normal to the edge. This suggests upwinding $\bar{u}$ based on the Riemann problem for Burgers' equations, namely,

$$\bar{u}_{i+1/2,j} = \begin{cases} \bar{u}^L & \text{if } \bar{u}^L \geq 0\,,\ \bar{u}^L + \bar{u}^R \geq 0 \\ 0 & \text{if } \bar{u}^L < 0\,,\ \bar{u}^R > 0 \\ \bar{u}^R & \text{otherwise} \end{cases}$$

(We suppress the $i+\frac{1}{2},j$ spatial indices on left and right states here and for the remainder of the discussion.) We now upwind U based on $\bar{u}$:

$$U_{i+1/2,j} = \begin{cases} U^L & \text{if } \bar{u}_{i+1/2,j} > 0 \\ U^R & \text{if } \bar{u}_{i+1/2,j} < 0 \\ \tfrac{1}{2}(U^L + U^R) & \text{if } \bar{u}_{i+1/2,j} = 0 \end{cases}$$

Note that the form of the differencing in (3.4) requires a value for $U_{i+1/2,j}$ even in "sonic" cases in which $\bar{u}_{i+1/2,j} = 0$.

The Godunov method is an explicit difference scheme and, as such, requires a time-step restriction. A linear, constant-coefficient analysis shows that we must require

$$\max_{ij}\left(\frac{\bar{u}_{ij}\Delta t}{J_{ij}}\,,\ \frac{\bar{v}_{ij}\Delta t}{J_{ij}}\right) \leq 1 \qquad (3.6)$$

for stability. The time-step restriction of the Godunov method is used to set the time step for the overall algorithm.

Discretization of the projection

In this section a numerical procedure is described for decomposing the intermediate velocity field U^* into its divergence-free and gradient components. Discrete vector decompositions of this type typically require that the difference schemes used to approximate the divergence and gradient yield skew adjoint operators over appropriate finite dimensional inner product spaces of discrete scalar and vector fields. This is

analogous to the situation in the continuous case when the vector and scalar fields have square integrable first order partial derivatives and satisfy specific conditions on the boundary of the domain. The decomposition considered here follows the finite difference Galerkin formulation used by Stephens et. al. [10]. In this approach, the divergence-free velocity component is determined directly by a Galerkin procedure using a local basis for the subspace of discretely divergence-free vector fields. An alternative procedure would be to compute the gradient component directly, with appropriate boundary conditions for this component. This approach for computing the decomposition has been used, for example, by van Kan [4], Chorin [5], and Kim and Moin [7].

The discrete divergence is defined on the dual grid system of Figure 1 by transforming to computational space and using conventional difference approximations. Thus, $\nabla\cdot U \simeq DU \equiv \overline{D}\overline{U}$, where $\overline{D}$ is a centered approximation to $\nabla_{\Xi}\cdot$ defined by

$$[\overline{D}\overline{U}]_{i+\frac{1}{2},j+\frac{1}{2}} \equiv \tfrac{1}{2}[(\overline{u}_{i+1,j+1}-\overline{u}_{i,j+1}) + (\overline{u}_{i+1,j}-\overline{u}_{ij}) + (\overline{v}_{i+1,j+1}-\overline{v}_{i+1,j}) + (\overline{v}_{i,j+1}-\overline{v}_{ij})]. \quad (4.1)$$

Recall that $\overline{U}_{ij} = T_{ij}U_{ij}$, where the matrices T_{ij} are evaluated using the finite difference approximations described in the previous section. These difference approximations were chosen to ensure that a uniform vector field, U_{∞}, will satisfy $DU_{\infty} = 0$, regardless of the grid being used.

We now define a discrete gradient operator that is numerically consistent with the pressure gradient term in (1.3) and is skew adjoint to D. Consider a domain covered by the staggered grid system with the indices $i=0$, $i=I$, $j=0$, and $j=J$ corresponding to the boundaries of the domain in physical space. On this mesh, $\overline{D}$ satisfies the summation-by-parts identity

$$\sum_{i=0}^{I-1}\sum_{j=0}^{J-1}[(\overline{D}\overline{U})\phi]_{i+\frac{1}{2},j+\frac{1}{2}} = -\sum_{i=0}^{I}\sum_{j=0}^{J}\overline{U}_{ij}\cdot[\overline{G}(E\phi)]_{ij} \quad (4.2)$$

where

$$(\overline{G}\phi)_{ij} = \tfrac{1}{2}\begin{bmatrix}\phi_{i+1/2,j+1/2}-\phi_{i-1/2,j+1/2}+\phi_{i+1/2,j-1/2}-\phi_{i-1/2,j-1/2}\\ \phi_{i+1/2,j+1/2}-\phi_{i+1/2,j-1/2}+\phi_{i-1/2,j+1/2}-\phi_{i-1/2,j-1/2}\end{bmatrix}$$

and $E\phi$ is the extension of ϕ by zero, (i.e. $(E\phi)_{i+\frac{1}{2},j+\frac{1}{2}} = \phi_{i+\frac{1}{2},j+\frac{1}{2}}$ for $i=1,\ldots,I$; $j=1,\ldots,J$ and $E\phi=0$ elsewhere). Note that the operator $\overline{G}$ is a centered difference approximation to ∇_{Ξ} . The identity (4.2) and (4.1) imply that

$$\sum_{i=0}^{I-1}\sum_{j=0}^{J-1}[(DU)\phi]_{i+\frac{1}{2},j+\frac{1}{2}} = -\sum_{i=0}^{I}\sum_{j=0}^{J}U_{ij}\cdot[T^t\overline{G}(E\phi)]_{ij} \quad (4.3)$$

The discrete gradient, G defined by

$$(G\phi)_{ij} \equiv T_{ij}^t[\overline{G}(E\phi)]_{ij} \quad (4.4)$$

represents a centered difference approximation to $T^t\nabla_{\Xi}\phi$ at interior nodes $i=1,\ldots,I-1$; $j=1,\ldots,J-1$. Furthermore, it follows from (4.3) and (4.4) that G and D are skew adjoint with respect to the spaces and inner products defined as follows. Let V denote the space of discrete vectors $\{U_{ij} : i=0,\ldots,I;\ j=0,\ldots,J\}$ and W the space of discrete scalars

$$\{\phi_{i+\frac{1}{2},j+\frac{1}{2}} : i=0,\ldots,I-1;\ j=0,\ldots,J-1\}$$

with inner products

$$(\phi,\psi)_W \equiv \sum_{i=0}^{I-1}\sum_{j=0}^{J-1}\phi_{i+\frac{1}{2},j+\frac{1}{2}}\psi_{i+\frac{1}{2},j+\frac{1}{2}}$$

and

$$(U,V)_V \equiv \sum_{i=0}^{I}\sum_{j=0}^{J}U_{ij}\cdot V_{ij}$$

on W and V, respectively. Then

$$(DU,\phi)_W = -(U,G\phi)_V \quad (4.5)$$

for all $U\in V$ and $\phi\in W$.

The specific form of the discrete decomposition depends on the boundary conditions for the problem under consideration. In this paper, we consider a class of problems for which the velocity is specified on a portion of the boundary, Γ_D, while the remainder of the boundary represents an outflow condition. Discrete Galerkin projections for problems of this type with the outflow modeled using homogeneous Neumann conditions on the velocity have been considered by Solomon and Szymczak [11]. In the formulation of [11], the specified Dirichlet data must satisfy compatibility conditions associated with the discrete divergence condition. The present treatment of the outflow boundary differs from that of [11] in that no conditions are explicitly imposed on the velocity at an outlet and there are no compatibility conditions on the specified data. The present treatment is analogous to imposing "natural" boundary conditions in a variational form for the projection.

The problem can be reduced to one with homogeneous data on the Dirichlet boundary by subtracting a boundary mesh vector $V_B \in V$ satisfying the specified Dirichlet data and $DV_B = 0$. A procedure for computing such boundary mesh vectors is described in [10, 11]. Since the intermediate velocity U^* satisfies the Dirichlet conditions, it follows that

$$U^*-V_B \in V^0 \equiv \{V\in V : V=0 \text{ on } \Gamma_D\} .$$

To obtain an orthogonal decomposition of V^0, we apply (4.5) to $U\in V^0$ to obtain

$$(DU,\phi)_W = -(U,G^0\phi)_V$$

where G^0 is defined to be zero on the Dirichlet boundary and given by (4.4), elsewhere. We therefore have the following direct sum decomposition of V^0

$$V^0 = D + G \quad (4.6)$$

where D = ker D and G = range G^0. A local basis for the subspace **D** is given by

$$\{\Psi^{k+\frac{1}{2},l+\frac{1}{2}} : (k,l) \in \mathbf{I}\}$$

where **I** is a set of indices defined by

$$\mathbf{I} = \{(i,j) : i=-1,\ldots,I,\ j=-1,\ldots,J \text{ and}$$
$$X_{i+i_1,j+j_1} \notin \Gamma_D \text{ for } i_1=0,1;\ j_1=0,1\}$$

and the mesh vectors $\Psi^{k+\frac{1}{2},l+\frac{1}{2}}$ are defined by

$$T_{ij}\Psi_{ij}^{k+\frac{1}{2},l+\frac{1}{2}} = \begin{cases} ((-1)^{l-j},(-1)^{k-i+1}) & \text{for } i=k,k+1; \\ & j=l,l+1 \\ (0,0) & \text{for all other } i,j \end{cases}$$

In the above, the index $k+\frac{1}{2},l+\frac{1}{2}$ corresponds to the cell that forms the support of the particular basis vector, and it is understood that each basis vector is an element of $\mathbf{V}^0$ by restriction where necessary.

To compute the projection of $U^* \in \mathbf{V}$ we note that from (4.6) it follows that $U^* - V_B = U_d + G^0\phi$ where $\phi \in \mathbf{W}$ and

$$U_d = \sum_{(i,j)\in\mathbf{I}} \alpha_{i+\frac{1}{2},j+\frac{1}{2}} \Psi^{i+\frac{1}{2},j+\frac{1}{2}} .$$

The coefficients $\alpha_{i+\frac{1}{2},j+\frac{1}{2}}$ are determined by solving the linear system

$$\sum_{(i,j)\in\mathbf{I}} \alpha_{i+\frac{1}{2},j+\frac{1}{2}} (\Psi^{i+\frac{1}{2},j+\frac{1}{2}}, \Psi^{k+\frac{1}{2},l+\frac{1}{2}})_{\mathbf{V}} =$$
$$(U^* - V_B, \Psi^{k+\frac{1}{2},l+\frac{1}{2}})_{\mathbf{V}} \qquad (4.7)$$

for all $(k,l) \in \mathbf{I}$. Note that the boundary mesh vector V_B is not unique, however, the sum $V_B + U_d$ is uniquely determined regardless of the choice of V_B. Therefore we can write $\mathbf{P}U^* = V_B + U_d$.

The linear system (4.7) has an algebraic structure of the type associated with a nine point discretization of the transformed Laplacian. This system is solved using a preconditioned conjugate gradient algorithm with a modified MILU(0) preconditioner. This step comprises the bulk of the computational work of the algorithm.

Numerical results

In this section we present computational results illustrating the performance of the method. The first example is for flow in a channel with a constriction. The constriction is given by a smooth Gaussian profile which, at its maximum extent, reduces the width of the channel by a factor of 2. A 400×50 grid was generated using a biharmonic grid generation algorithm [12]. No clustering terms were used so the grid is essentially uniformly distributed.

Computational results for parabolic inflow with no slip walls are presented in Figs. 2-4 for R_e = 50, 500 and 5000. Here R_e is based on the maximum inflow velocity and the inlet channel width. For R_e = 50 the flow quickly converges to the steady profile shown in Fig. 2 which shows a small recirculation region behind the constriction. For R_e = 500, shown in Fig. 3, the recirculation region has become much larger than in the previous case, extending approximately 7 "bump-heights" downstream before reattaching. A second separated region has also formed along the top of the channel. Similar phenomena were reported by Armaly et. al. [13] for the backward-facing step at a comparable Reynolds number. We note that this profile is still slowly changing after several thousand time steps; whether a steady state will eventually be reached or not is unknown.

In Fig. 4, we show a time sequence of the flow for R_e = 5000 after the initial transients have disappeared. This Reynolds number is well into the turbulent regime and the resulting flow is quite complex. The dominant features of the flow are the large vortices being alternately shed from the top and bottom walls. A number of smaller secondary structures are also apparent. The flow directly behind the constriction is particularly complex, involving a number of counter-rotating vorticies that participate in shedding cycle.

Our second example is flow over a cylinder. We specified uniform horizontal flow at the left, top and bottom boundary conditions corresponding to a cylinder pulled through quiescent fluid in a channel 8 cylinder diameters wide viewed in a frame of reference moving with the cylinder. We discretized a section of the channel 25 cylinder diameters long with a 600×160 grid. In this case the grid is given by an inverse Joukowski transformation from a rectangular computational space with a slit, again with no clustering of grid-points around the cylinder. Some minor modifications were made to the algorithm to enforce no flow boundary conditions along the cylinder. In Fig. 5, we show a time sequence for an established flow at R_e = 400. (The top and bottom halves are plotted separately causing a break in some of the contour lines along the centerline.) The computations exhibit the expected vortex street formed by the alternate shedding of vortices from the top and bottom of the cylinder. The numerical results provide good resolution of the flow with no sign of oscillations in spite of a cell-Reynolds-number greater than 20.

Assessing the computational efficiency of the algorithm requires some caution. The dominant cost in the algorithm is the solution of the linear system associated with the projection. This system is solved iteratively and the performance of the iterative method depends on a number of factors including the problem size, the complexity of the flow, the boundary conditions and the level of distortion of the grid. For the constricted channel problem described above the method required approximately 25 μsec per zone on a Cray-XMP using one processor. This figure is based on the time spent in the main integration loop during the first 20 time steps at Reynolds number 500 and does

not include initialization, grid generation and other start-up costs. This particular case is ideally suited to the method and typical timings are likely to be somewhat higher.

Conclusions

In this paper we have described a numerical method for solving the incompressible Navier-Stokes equations on a logically-rectangular quadrilateral grid. The method uses a second-order projection formulation and incorporates a Godunov-type discretization of the convective terms that is second-order accurate for smooth flow and is sufficiently robust to treat strongly sheared flows without loss of stability or oscillations independent of Reynolds number. In future work we plan to use this integration scheme as the basis for an adaptive mesh refinement algorithm in which regions where additional accuracy is required are locally refined.

References

1. J. B. Bell, P. Colella, and H. M. Glaz, "A Second-Order Projection Method for Viscous, Incompressible Flow," in *AIAA 8th Computational Fluid Dynamics Conference*, Honolulu, Hawaii, June 9-11, 1987.
2. J. B. Bell, P. Colella, and H. M. Glaz, "A Second-Order Projection Method for the Incompressible Navier-Stokes Equations," *J. Comp. Phys.*, to appear.
3. J. B. Bell, H. M. Glaz, J. M. Solomon, and W. G. Szymczak, "Application of a Second-Order Projection Method to the Study of Shear Layers," *11th Inbternational Conference on Numerical Methods in Fluid Dynamics*, Williamsburg, VA, June 27-July 1, 1988.
4. J. Van Kan, "A Second-Order Accurate Pressure-Correction Scheme for Viscous Incompressible Flow," *SIAM J. Sci. Stat. Comput.*, vol. 7, pp. 870-891, July 1986.
5. A. J. Chorin, "On the Convergence of Discrete Approximations to the Navier-Stokes Equations," *Math. Comp.*, vol. 23, pp. 341-353, April 1969.
6. R. Temam, *Navier-Stokes Equations*, Elsevier Science Publishers, Amsterdam, 1984.
7. J. Kim and P. Moin, "Application of a Fractional-Step Method for Incomressible Navier-Stokes Equations," *J. Comput. Phys.*, vol. 59, pp. 308-323, 1985.
8. P. Colella, "A Multidimensional Second Order Godunov Scheme for Conservation Laws," LBL-17023, Lawrence Berkeley Laboratory, to appear in J. Comp. Phys..
9. B. Van Leer, "Multidimensional Explicit Difference Schemes for Hyperbolic Conservation Laws," *Computing Methods in Applied Sciences and Engineering, VI*, pp. 493-499, Elsevier Science Publishers, 1984.
10. A. B. Stephens, J. B. Bell, J. M. Solomon, and L. B. Hackerman, "A Finite Difference Galerkin Formulation of the Incompressible Navier-Stokes Equations," *J. Comp. Phys.*, vol. 53, pp. 152-172, Jan. 1984.
11. J. M. Solomon and W. G. Szymczak, "Finite Difference Solutions for the Incompressible Navier-Stokes Equations using Galerkin Techniques," *Fifth IMACS International Symposium on Computer Methods for Partial Differential Equations*, Lehigh University, June 19-21, 1984.
12. J. B. Bell, G. R. Shubin, and A. B. Stephens, "A Segmentation Approach to Grid Generation Using Biharmonics," *J. Comp. Phys.*, vol. 47, pp. 463-472, 1982.
13. B. F. Armaly, F. Durst, J. C. F. Pereira, and B. Schonung, "Experimental and theoretical investigation of backward-facing step flow," *J. Fluid Mech.*, vol. 127, pp. 473-496, 1983.

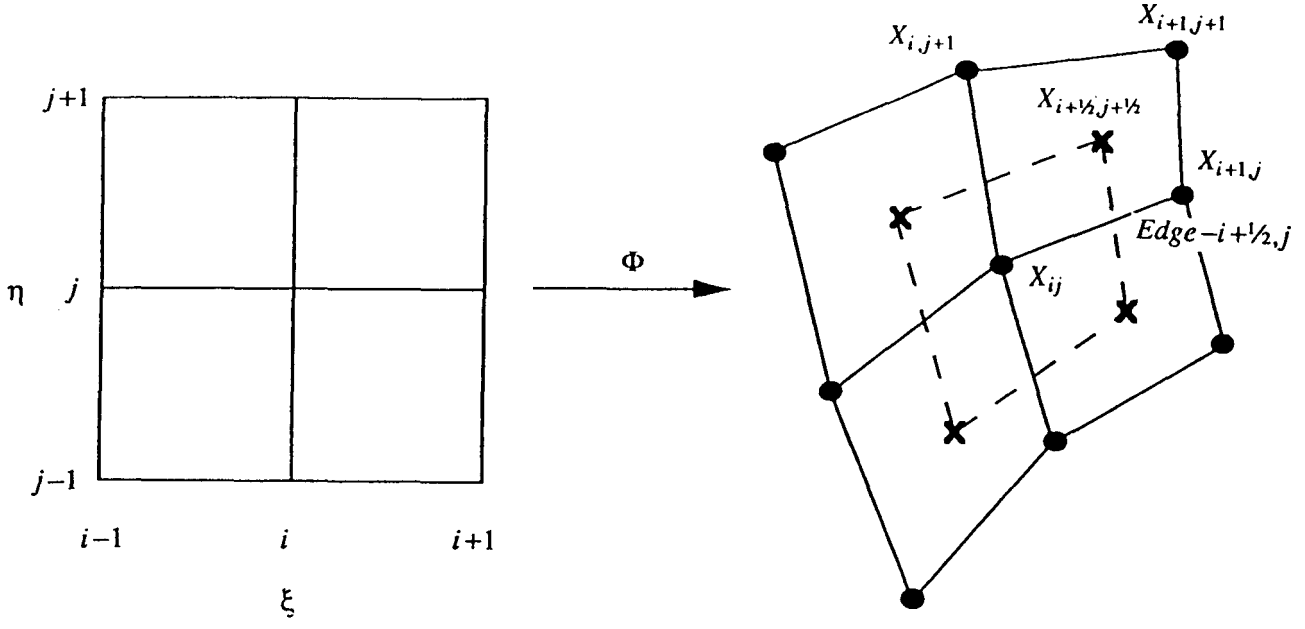

Fig. 1. Staggered grid structure.

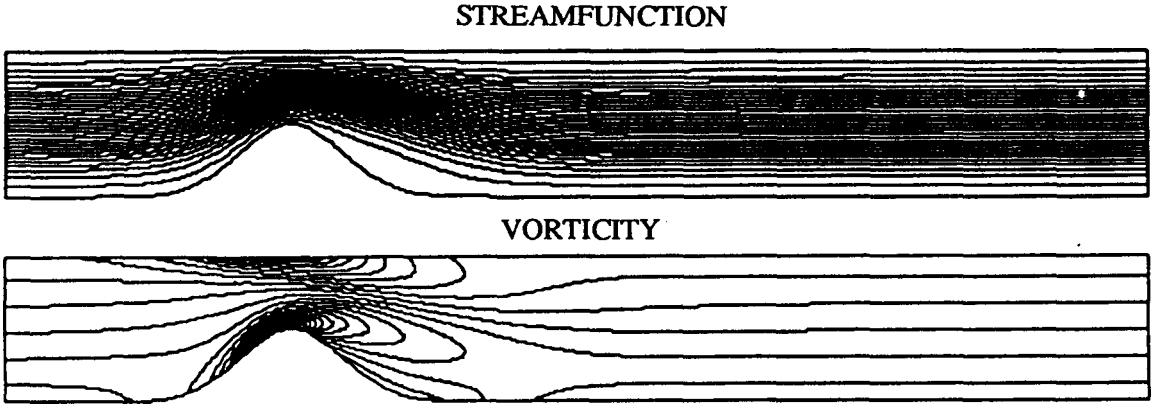

Fig. 2. Steady flow in constricted channel at $R_e = 50$.

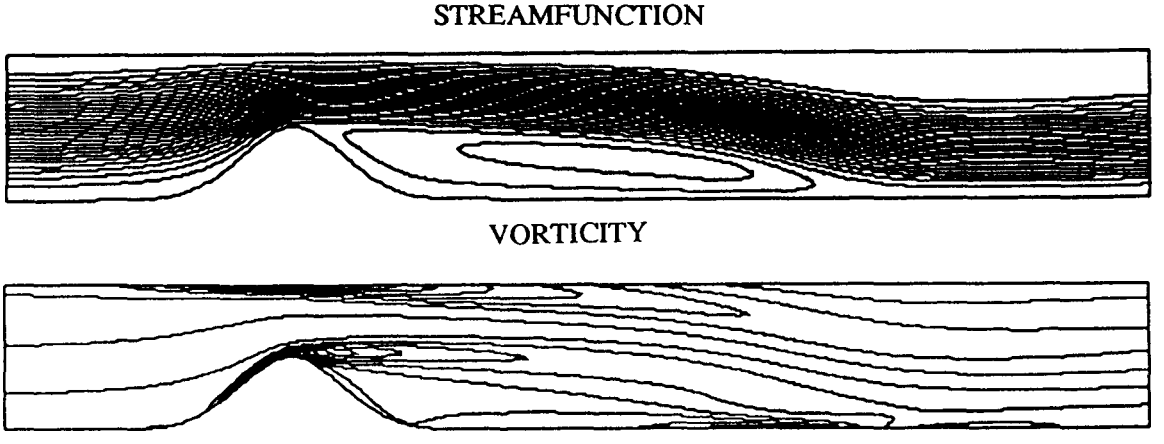

Fig. 3. Flow in constricted channel at $R_e = 500$.

TIME = 16.7

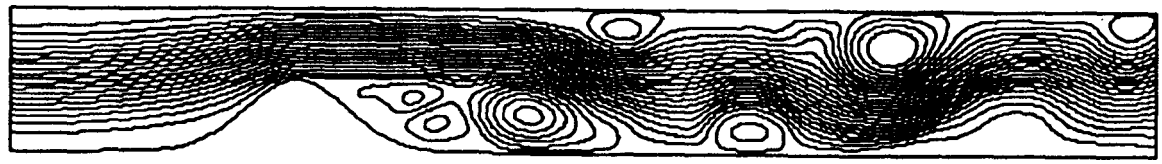

TIME = 17.9

TIME = 19.0

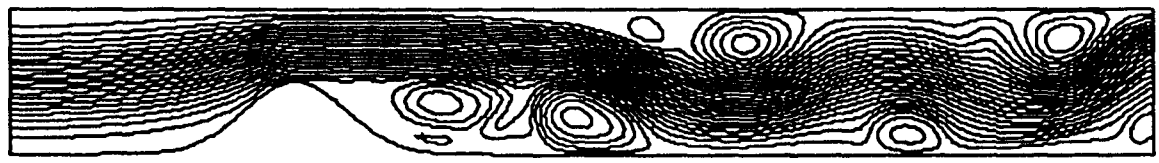

TIME = 20.2

Fig. 4a. Time sequence of flow in constricted channel at R_e = 5000 -- streamfunction

TIME = 16.7

TIME = 17.9

TIME = 19.0

TIME = 20.2

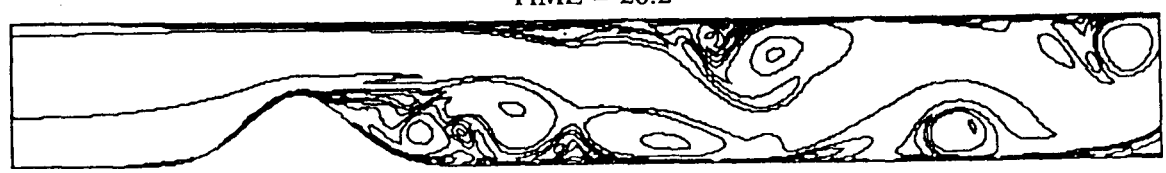

Fig. 4b. Time sequence of flow in constricted channel at R_e = 5000 -- vorticity

STREAMFUNCTION

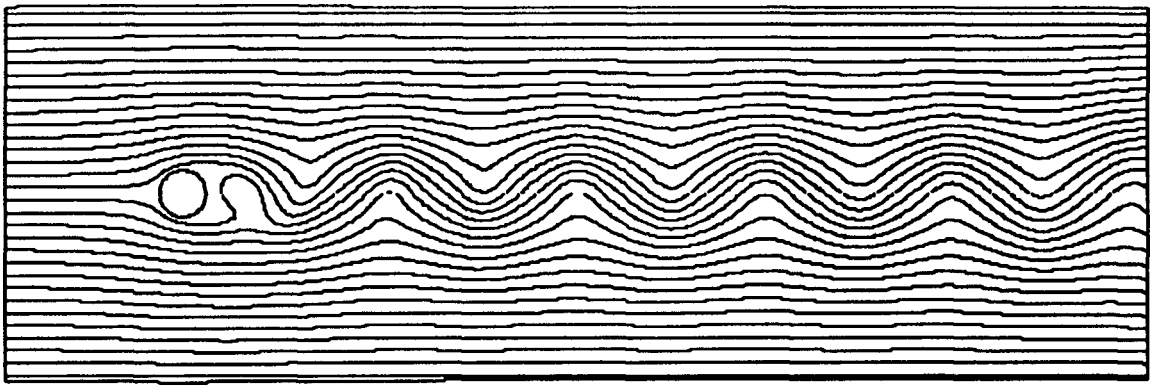

VORTICITY

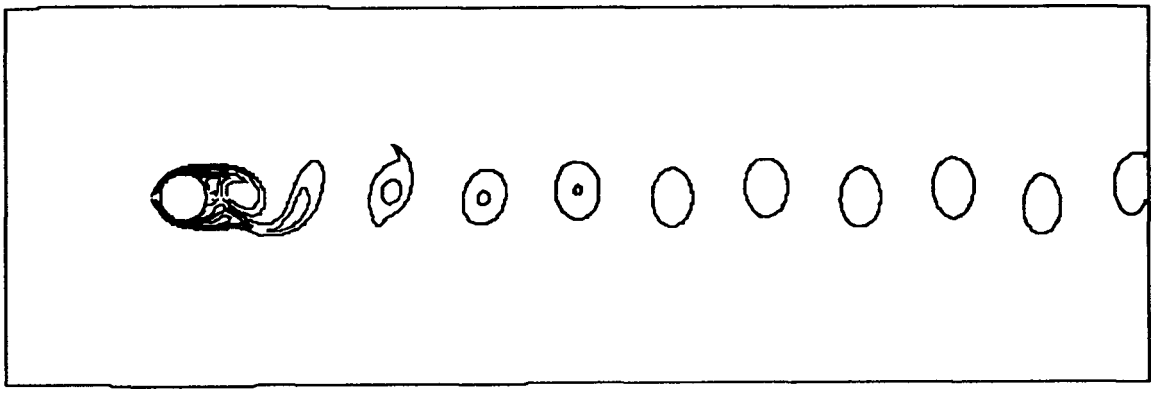

Fig. 5. Flow past a cylinder at $R_e = 400$.